Altered expression of FHL1, CARP, TSC-22 and P311 provide insights into complex transcriptional regulation in pacing-induced atrial fibrillation

Chien-Lung Chen, Jiunn-Lee Lin, Ling-Ping Lai, Chun-Hsu Pan, Shoei K. Stephen Huang, Chih-Sheng Lin

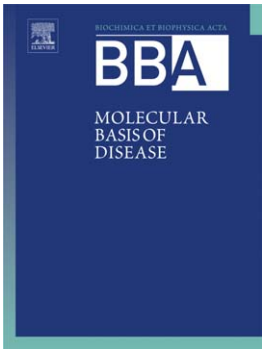

Altered expression of FHL1, CARP, TSC-22 and P311 provide insights into complex transcriptional regulation in pacing-induced atrial fibrillation

Chien-Lung Chen, Jiunn-Lee Lin, Ling-Ping Lai, Chun-Hsu Pan, Shoei K. Stephen Huang, Chih-Sheng Lin

PII: S0925-4439(06)00231-6
DOI: doi: 10.1016/j.bbadis.2006.10.017
Reference: BBADIS 62658

To appear in: *BBA - Molecular Basis of Disease*

Received date: 13 July 2006
Revised date: 23 October 2006
Accepted date: 24 October 2006

Please cite this article as: Chien-Lung Chen, Jiunn-Lee Lin, Ling-Ping Lai, Chun-Hsu Pan, Shoei K. Stephen Huang, Chih-Sheng Lin, Altered expression of FHL1, CARP, TSC-22 and P311 provide insights into complex transcriptional regulation in pacing-induced atrial fibrillation, *BBA - Molecular Basis of Disease* (2006), doi: 10.1016/j.bbadis.2006.10.017

Altered expression of FHL1, CARP, TSC-22 and P311 provide insights into complex transcriptional regulation in pacing-induced atrial fibrillation

Chien-Lung Chen [a], Jiunn-Lee Lin [b], Ling-Ping Lai [b], Chun-Hsu Pan [a], Shoei K. Stephen Huang [c], Chih-Sheng Lin [a,*]

[a] Department of Biological Science and Technology, National Chiao Tung University, Hsinchu 300, Taiwan

[b] Division of Cardiology, Department of Internal Medicine, National Taiwan University Hospital, Taipei 100, Taiwan

[c] Division of Cardiology, Department of Internal Medicine, China Medical University Hospital, Taichung 404, Taiwan

*** Corresponding author:**

Chih-Sheng Lin, Ph.D.

Department of Biological Science and Technology,

National Chiao Tung University,

75 Po-Ai Street, Hsinchu 30005, Taiwan, ROC

Tel: 886-3-5131338 Fax: 886-3-5729288

E-mail: lincs.biotech@msa.hinet.net

Abstract

Atrial fibrillation (AF) is the most common progressive disease in patients with cardiac arrhythmia. AF is accompanied by complex atrial remodeling and changes in gene expression, but only a limited number of transcriptional regulators have been identified. Using a low-density cDNA array, we identified 31 genes involved in transcriptional regulation, signal transduction or structural components, which were either significantly upregulated or downregulated in porcine atria with fibrillation (induced by rapid atrial pacing at a rate of 400-600 bpm for 4 weeks that was then maintained without pacing for 2 weeks). The genes for four and a half LIM domains protein-1 (*FHL1*), transforming growth factor-β (TGF-β)-stimulated clone 22 (*TSC-22*), and cardiac ankyrin repeat protein (*CARP*) were significantly upregulated, and chromosome 5 open reading frame gene 13 (*P311*) was downregulated in the fibrillating atria. FHL1 and CARP play important regulatory roles in cardiac remodeling by transcriptional regulation and myofilament assembly. Induced mRNA expression of both *FHL1* and *CARP* was also observed when cardiac H9c2 cells were treated with an adrenergic agonist. Increasing TSC-22 and marked P311 deficiency could enhance the activity of TGF-β signaling and the upregulated *TGF-β1* and *-β2* expressions were identified in the fibrillating atria. These results implicate that observed alterations of underlying molecular events were involved in the rapid-pacing induced AF, possibly via activation of the β-adrenergic and TGF-β signaling.

Keywords: Atrial fibrillation; Low-density cDNA array; Transcriptional regulator; Transforming growth factor-β signaling.

1. Introduction

Atrial fibrillation (AF), the most common sustained arrhythmia, causes progressive alterations in atrial electrical, contractile and structural properties, which are associated with changes in cardiac gene expression [1,2]. Recent studies have focused on the molecular basis of atrial remodeling using candidate gene and genome-wide approaches in AF patients [3-5]. Gene expression profiling studies on dedifferentiation [3], apoptosis [5], fibrosis and thromboembolic events [4] have highlighted the complex regulation of gene expression during AF formation and maintenance. However, thus far, transcriptional regulators involved in regulating transcription in AF have been proposed [6], but attempts to identify the regulators have been lacking. Activation of transcriptional regulators during AF may coordinately lead to sequential transcriptional control events that regulate the phenotype of cardiomyocytes in response to AF disease conditions [6]. In fact, AF is often associated with other cardiovascular diseases such as hypertension, thyrotoxic heart disease, coronary artery disease, rheumatic valve disease, and heart failure [7]. Moreover, changes in gene expression in clinical AF may be the result of AF combined with other underlying heart diseases [4]. Therefore, functional studies of transcriptional regulators in rapid pacing-induced AF or transgenic animal AF models [8] may clarify the underlying molecular mechanisms of AF because the potential confounding effects of other underlying heart diseases have been eliminated.

In the present study, we investigated 84 candidate genes specifically associated with fibrillating atria of a porcine AF induced by rapid atrial pacing using a low-density cDNA array. Three genes, four and a half LIM domains protein-1 (*FHL1*), transforming

growth factor beta-stimulated clone 22 (*TSC-22*) and cardiac ankyrin repeat protein (*CARP*), encoding transcriptional regulators, were significantly upregulated, and chromosome 5 open reading frame gene 13 (*P311*), an anti-fibrotic gene, was downregulated in the fibrillating atria. Along with confirmation of the selected genes for differential expression profiles, the further identification of protein expression and implicated mechanism in the fibrillating atria were subsequently evaluated. The results provide more insights into the underlying molecular events in pacing-induced AF and evidence of complex transcriptome changes that may accompany AF development.

2. Materials and methods

2.1. AF induced by rapid atrial pacing

A porcine model of AF was used as described previously [9]. Eighteen adult Yorkshire-Landrace strain pigs were used (12 in the AF group and 6 in the sham control group), with mean body weight 62 ± 5 kg. In this study, six pigs in the AF group were added besides the specimens of 6 AF and 6 sham control that were sampled in our previous study [10]. The experimental protocol conformed to the Guide for the Care and Use of Laboratory Animals (NIH Publication No. 85-23, revised 1996) and was approved by the Institutional Animal Care and Use Committee of the National Taiwan University College of Medicine. All pigs were provided by the Animal Technology Institute in Taiwan (ATIT) and housed at the animal facility in the ATIT. Each animal was transvenously implanted with either a high-speed atrial pacemaker (Itrel-III; Medtronic Inc., Minneapolis, MN) for the AF group or an inactive pacemaker for the sham control group (i.e., sham hearts maintained normal sinus rhythm, SR). The atrial

pacing lead (Medtronic) was inserted through the jugular vein and screwed to the right atrium. The atrial high-speed pacemaker was programmed to a rate of 400-600 beats per min for 4 weeks in the AF group. After continuous pacing, the atrial pacemaker was turned off and the animals remained in AF. The animals were sacrificed 2 weeks after the pacemaker was turned off, and thus the total duration of atrial depolarization was 6 weeks. In the sham control group, the pacemaker remained off for the entire 6 weeks after implantation.

2.2. Tissue processing

The pigs were anaesthetized and sacrificed at the end of the experimental period. The right atrial appendages (RAA) and left atrial appendages (LAA) were excised and immediately frozen in liquid nitrogen and then stored at –80°C until use for RNA or protein extraction for later experiments.

2.3. RNA isolation

Total RNA was extracted and quantified from the pig LAA and RAA according to our previous report [11]. In brief, 200 mg of atrial tissue was homogenized on ice by a rotor-stator-type tissue homogenizer in 1 ml TRIzol reagent (GIBCO BRL, Gaithersburg, MD). Cellular debris was removed by centrifugation for 10 min at 12,000 × *g* at 4°C, and RNA was precipitated by adding equal volumes of isopropanol and then washing with 75% ethanol. The resultant RNA was further purified with the RNeasy Midi kit (Qiagen, Valencia, CA) according to the manufacturer's instructions. The amount of total RNA was determined spectrophotometrically at 260 nm, and the integrity was confirmed by analysis on a denaturing agarose gel. The RNA was used in

the cDNA microarray and quantitative real-time RT-PCR analysis.

2.4. Specialized AF Chip design and preparation

A total of 84 gene sequences were selected for a low-density cDNA array, named the AF Chip. Selection of these genes was based on the following three considerations: the gene had been reported to be associated with a cardiomyopathy [12], the gene was significantly and differentially expressed in fibrillating tissue of a rapid pacing-induced AF model in our previous report on a microarray containing 6,032 human cDNA clones (UniversoChip, AsiaBioinnovations, Newark, CA) [10], and the gene clone was available from the IMAGE consortium (Open Biosystems, Huntsville, AL). All symbols and accession numbers of the selected genes used in the AF Chip are shown in Fig. 1. Additionally, two control cDNAs, glyceraldehyde-3-phosphate dehydrogenase (*GAPDH*) and β-tubulin, as well as pUC19, were included in the chip. The selected clones were purchased from IMAGE consortium, and the sequences were verified in our laboratory. The clones were amplified using PCR with 36 cycles of a denaturing temperature of 95°C for 30 s, annealing temperature of 55°C for 30 s, and extension temperature of 72°C for 45 s. The commercial primers for amplification were as follows: T7 primer (5'-TAA TAC GAC TCA CTA T AG GG-3'), Sp6 primer (5'-CAT ACG ATT TAG GTG ACA CTA TAG-3'), T3 primer (5'-AAT TA A CCC TCA CTA AAG-3'), M13 forward primer (5'-GTA AAA CGA CGG CCA G-3'), and M13 reverse primer (5'-CAG GAA ACA GCT ATG AC-3') (Invitrogen, Carlsbad, CA). After amplification, the quality and specificity of the PCR products were confirmed by agarose gel electrophoresis.

PCR-amplified DNA products were mixed with dimethyl sulfoxide (1:1, v/v) and

then spotted onto amino-coated glass slides (TaKaRa Mirus Bio Inc., Madison, WI) using a robotics SpotArray 24 (PerkinElmer Life Sciences, Boston, MA). To evaluate the reliability of the AF Chip, PCR-amplified DNA products were spotted in duplicate onto a slide. Spotted DNA was crosslinked and denatured according to the manufacturer's instructions (Takara Mirus Bio Inc., http://www.takaramirusbio.com).

2.5. Hybridization and imaging of fluorescently labeled cDNA

Twenty μg of total RNA extracted from the SR and AF subjects was reverse-transcribed with an oligo-dT primer to prepare fluorophore-labeled SR and AF cDNA with Cyanine-3 dUTP (Cy3) and Cyanine-5 dUTP (Cy5) (PerkinElmer Life Science, Boston, MA), respectively. Fluorophore-labeled cDNA pairs were precipitated together with ethanol and purified using Microcon YM-30 purification columns (Millipore, Bedford, MA). The labeled cDNAs were resuspended in the hybridization buffer of 20% formamide, 5× SSC, 0.1% SDS and 0.1 mg/ml salmon sperm DNA (Ambion, Austin, TX), and then denatured by heating at 95°C for 3 min. The mixture of labeled cDNA pairs was applied to the AF Chips under a 22-mm^2 cover slip and allowed to hybridize for 16 h at 55°C in a hybridization chamber (GeneMachines, San Carlos, CA). The chips were washed at 45°C for 10 min in 2× SSC, 0.1% SDS, followed by two washes at room temperature in 1× SSC (10 min) and 0.2× SSC (15 min). After hybridization, the slides were scanned with a dual-laser scanner GenePix 4000B at 10-μm resolution (Axon Instruments Inc., Union, CA). Results of the competitive hybridization were imaged at different photomultiplier settings to yield a balanced and applicable signal. Spots with saturated signal intensity or with signal less than background were excluded from the final data set. The data were converted from image

158 to signal using GenePix Pro 4.1 software (Axon Instruments Inc.) for further statistical
159 analysis.

160 *2.6. Data analysis and gene ontology*

161 The fluorescence intensity of the local mean background was calculated for each
162 spot, and we accepted only those cDNA spots with a fluorescence signal intensity more
163 than the mean local background plus 2 standard deviations (SD) and greater than the
164 intensity of the negative control. The signals from all the experimental arrays were
165 normalized based on the *GAPDH* probe sets in which the average signal from *GAPDH*
166 (as an internal control) was defined as unchanged. On the same AF Chip, the two
167 intensity values of the duplicate cDNA clone spots were averaged and used to determine
168 the ratio between the AF and sham control subjects (i.e., the ratio of Cy5/Cy3
169 intensities). Genes were classified as differentially expressed when the value of the
170 mean ratios was ≥ 1.5 or ≤ 0.67. Functional classification of the differentially expressed
171 genes was according to the GeneCards web site (http://www.genecards.org/
172 index.shtml) and the Gene Ontology Consortium (http://www.geneontology.org).

173 *2.7. Quantitative real-time reverse transcription-PCR*

174 SYBR Green quantitative real-time reverse transcription-PCR (RT-PCR) was
175 performed on the genes *FHL1*, *TSC-22*, *CARP*, *P311, TGF-β1, -β2, -β3* and *GAPDH* (as
176 an internal control) to confirm the results obtained by the AF Chip and *TGF-β* isoforms
177 mRNA expression. The specific forward and reverse primers were designed with
178 Primer Express software (PE Applied Biosystems, Foster, CA) (Table 1). The cDNA
179 was synthesized by extension with oligo (dT) primer at 42°C for 60 min in a 25-μl

reaction containing 5 μg total RNA, 1× First-Strand Buffer (75 mM KCl, 3 mM $MgCl_2$, 50 mM Tris-HCl, pH 8.3), 8 mM DTT, 10 μM dNTPs, 20 U RNase inhibitor, and 200 U Superscript II reverse transcriptase (Invitrogen). For each selected gene, the primer sets were tested for quality and efficiency to ensure optimal amplification of the samples. Real-time RT-PCR was performed at 1, 1/4, 1/16, 1/64, 1/128, and 1/512 dilution of the synthetic cDNAs to define relative fold changes. Real-time RT-PCR reactions contained 12.5 μl SYBR Green PCR master mix (PE Applied Biosystems), 2 μl forward primer (10 μM), 2 μl reverse primer (10 μM), 3 μl cDNA, and 5.5 μl distilled water. All PCR reactions were carried out in triplicate with the following conditions: 2 min at 50°C, 10 min at 95°C, followed by 40 cycles of 15 s at 95°C, 30 s at 57°C, and 30 s at 60°C in a 96-well optical plate (PE Applied Biosystems) in the ABI 7000 Sequence Detection System (PE Applied Biosystems). A PCR reaction without cDNA was performed as a template-free negative control. According to the instructions of PE Applied Biosystems, the expression of each gene was quantified as ΔC_t (C_t of target gene – C_t of internal control gene) using *GAPDH* as the control and applying the formula $2^{-\Delta\Delta Ct}$ to calculate the relative fold changes [13].

2.8. Protein preparation and western blot analysis

Western blotting was performed to determine the protein levels of FHL1 and CARP in the atrial AF and SR tissues. Frozen atrial tissues (about 200 mg) were homogenized in 1 ml of ice-cold lysis buffer containing 20 mM Tris-HCl, pH 7.6, 1 mM dithiothreitol, 200 mM sucrose, 1 mM EDTA, 0.1 mM sodium orthovanadate, 10 mM sodium fluoride, 0.5 mM phenylmethylsulfonyl fluoride and 1% (v/v) Triton X-100. The homogenates were then centrifuged at 10,000 × *g* for 30 min at 4°C. Supernatants

were collected and protein concentration was measured with the Bio-Rad protein assay (Bio-Rad Laboratories, Hercules, CA). Equal amounts of protein (20 μg /lane) were separated on 10% polyacrylamide gels by SDS-PAGE and transferred onto polyvinylidene fluoride membranes (Millipore) at 50 mA for 90 min in a semi-dry transfer cell (Bio-Rad). Membranes were blocked for 60 min in TBS (10 mM Tris-HCl, 0.15 M NaCl, pH 7.4) containing 5% nonfat dry milk with gentle shaking. Following three washes with TBS containing 0.1% (v/v) Tween-20 for 5 min, the membrane was incubated with anti-human FHL1 (1:5000), anti-human CARP (1:5000), or anti-human β-tubulin (1:5000; all three antibodies were from Santa Cruz Biotechnology, Santa Cruz, CA), and detected using horseradish peroxidase–conjugated anti-goat IgG and ECL western blotting detection reagents (Amersham Pharmacia Biotech, Little Chalfont, UK) according to the manufacturer's instructions. The images were scanned, and densities of each band were analyzed by Scion image software (National Institutes of Health, Bethesda, MD). The relative protein expression of FHL1 and CARP was normalized to β-tubulin expression.

2.9. Histological examination

Fresh tissues of atrial appendages were cut into 3-5 mm slices and fixed in 4% (v/v) formalin buffer containing 0.1 M sodium phosphate (pH 7.5) before paraffin embedding. Tissue blocks were treated into 6 μm sections and deparaffinized for Hematoxylin-eosin and Masson's trichrome blue staining.

2.10. Immunohistochemical assay

Immunohistochemical assay was performed on 6 μm sections that were rehydrated

and blocked with 10% (v/v) normal goat serum (Santa Cruz Biotechnology). Subsequently, the sections were incubated overnight at 4°C with anti-FHL1 or -CARP specific antibodies (Santa Cruz Biotechnology) in Tris-buffered saline (10 mM Tris-HCl, pH 8.0, 150 mM NaCl), followed by incubations with biotinylated secondary antibodies that were detected with streptavidin– horseradish peroxidase conjugates (Vectastain Elite ABC kit; Vector Laboratory, Burlingame, CA). Peroxidase activity was visualized with diaminobenzidine and hydrogen peroxide. For detection, a control was done by omitting the primary antibody to determine the nonspecific binding. Nuclei were counterstained with hematoxylin.

2.11. Cell culture and treatment

H9c2 cardiomyocytes (ATCC; CRL1446) were plated at 60% confluence in Dulbecco's Modified Eagle's Medium (DMEM) containing 10% fetal calf serum (FCS), 2 mM L-glutamine, 100 U/ml penicillin and 100 µg/ml streptomycin (growth-promoting medium). The medium was switched to DMEM containing 1% FCS for 48 h (differentiation-promoting medium) when the H9c2 cells had grown to 70-80% confluence. The cells were then treated with 1 µM angiotensin II (Ang II) (Sigma, St. Louis, MO), 10 µM isoproterenol (Sigma), 0.2 mM H_2O_2 (Merck, Darmstadt, Germany), or the same volume of Dulbecco's PBS (DPBS; control treatment). The treated cells were harvested 12 h after treatment, and total RNA was isolated as described above.

2.12. Semi-quantitative RT-PCR

Unique PCR primers specific for *FHL1* (5'-AGG GGA GGA CTT CTA CTG TGT

G-3' and 5'-CCA GAT TCA CGG AGC ATT TT-3'), *CARP* (5'-AAA TCA GTG CCC GAG ACA AG-3' and 5'-ATT CAA CCT CAC CGC ATC A-3') and *GAPDH* (5'-GGT GAT GCT GGT GCT GAG TA-3' and 5'-TTC AGC TCT GGG ATG ACC TT-3') were designed using PRIMER3 software (available online at http://frodo.wi.mit.edu/cgi-bin/primer3/primer3_www.cgi) and the nucleic acid sequence database from the National Center for Biotechnology Information (NCBI). Total RNA from H9c2 cells was prepared as described above. The cDNA was synthesized by Superscript II reverse transcriptase (Invitrogen) from 5 μg of total RNA. The PCR reaction contained 3 μl cDNA, 2 μl forward and reverse primers (10 μM), 5 μl 10× PCR buffer, 2 μl 10 mM dNTPs, 1 μl of 5 U/μl Taq polymerase (Promega, Madison, WI) and 37 μl distilled water in a total volume of 50 μl. DNA was amplified by an initial incubation at 94°C for 3 min followed by 25-30 cycles of 94°C for 30 s, 60°C for 30 s, 72°C for 30 s, and a final extension at 72°C for 6 min. The PCR products were separated by electrophoresis in a 2% agarose gel, visualized by ethidium bromide staining, and the band intensity was quantified using an image analyzer (Kodak DC290 Digital camera System; Eastman Kodak, Rochester, NY). The relative amount of mRNA was measured using densitometric analysis by Scion image (National Institutes of Health) and normalized to the level of *GAPDH* mRNA.

2.13. Statistical analysis

Experimental results are expressed as means ± SD. Data from the AF Chip, real-time RT-PCR, semi-quantitative RT-PCR and western blots were analyzed using the Student's *t* test. Differences with $P < 0.05$ were considered significant.

3. Results

3.1 Quality assessment of the AF Chip hybridization

In our previous study using a high-density cDNA microarray, many genes demonstrated marked expression changes in the fibrillating atria of a rapid pacing-induced AF model [10]. However, the genes involved in signal transduction and transcriptional regulation during AF have not been evaluated in detail. Therefore, we constructed a low-density cDNA array, the AF Chip, which included genes in these functional pathways and others to investigate changes in gene expression in atrial tissues during AF. The chip was fabricated with 84 AF or heart diseases-related genes mentioned in published papers, including our own previous report [10], to further analyze their relationship with AF.

To validate the reproducibility and quality of the AF Chip, we analyzed correlation factors from the intensity values of each gene in duplicated spots and replicated hybridizations. The scatter-plot analysis of the raw signal intensities of duplicated spots in a representative hybridization (Fig. 2A) fit a linear line with correlation factors of 0.985 and 0.981 in the Cy5 (in red; Fig. 2B) and Cy3 (in green; Fig. 2C) channels, respectively. In the AF Chip experiments, two independent hybridizations were performed for each sample, and the mean intensity values for each gene from one chip were plotted against those from the second chip. After normalization, the correlation factors of the 12 replicate hybridization data with Cy3 and Cy5 normalized intensities ranged from 0.921 to 0.993 (average of 0.964 in the Cy3 channel and 0.947 in the Cy5 channel). The results demonstrate that the AF Chip data were reproducible. Moreover, these high correlation factors indicate that the AF Chip was consistent and reliable.

3.2 Genes with altered expression in AF

Following competitive hybridization using labeled cDNAs from individual RAA tissues of AF and SR, the ratio of expression of each gene (Cy5 signal intensity in AF, and Cy3 signal intensity in SR) was averaged and evaluated by the Student's *t* test. The 31 genes with significantly altered mRNA expression in rapid-pacing induced AF were shown in Table 2. These genes were classified into seven functional categories according to the molecular and biological function of their encoded protein. The categories include transcription (4 genes), structural components (8), metabolism (4), signal transduction (3), cell proliferation (2), and others (10, including ESTs), among which, two genes encoding proteins associated with the myofibrillar apparatus, myosin regulatory light chain-2 (*MLC-2V*) and cysteine and glycine-rich protein 1 (*CSRP1*), showed a 4.4- and 2.6-fold increase in AF, respectively. Several genes encoding components of the extracellular matrix were differentially expressed in AF, like increased expression of spondin 1 (*SPON1*), fibronectin 1 (*FN1*), cadherin 2 (*CDH2*) and a disintegrin and metalloprotease domain 10 (*ADAM10*), and decreased expression of cartilage-associated protein (*CRTAP*) and matrix metalloproteinase 11 (*MMP-11*). Genes involved in signal transduction pathways, including calmodulin 2 (*CALM2*), beta-2 adrenergic receptor (β_2AR) and insulin-like growth factor binding protein 5 (*IGFBP5*), showed upregulation. Among the unclassified genes, the marked downregulation of *P311* in fibrillating atria is particularly interesting because of its putative anti-fibrotic function. There were four genes, *FHL1*, *CARP*, *TSC-22* and *TCEB1*, which encode transcriptional cofactors or modulators [14-17], that showed increased expression of between 1.6- and 3.2-fold ($P < 0.01$) (Table 2). They may contribute to the altered transcription processes involved in the complex remodeling

during AF, but, to the best of our knowledge, the transcriptional regulators associated with AF have not been well explored.

3.3 Validation of altered gene expression by quantitative real-time RT-PCR

Quantitative real-time RT-PCR was performed to validate the mRNA expression results of the AF Chip. We selected four differentially expressed genes *FHL1*, *TSC-22*, *CARP*, and *P311*. As mentioned above, *P311* was of particular interest because of its putative anti-fibrotic function, and *FHL1, TSC-22* and *CARP* were chosen for further study because these genes play regulatory roles in transcription and structural alterations in cardiomyocytes [15-17]. Total RNA extracted from the RAA and LAA of AF and SR model pigs was used in real-time RT-PCR, and the relative mRNA expression level of each gene was normalized to that of *GAPDH* mRNA. The relative *FHL1*, *TSC-22* and *CARP* mRNA expression levels in RAA with AF were significantly upregulated 5.1-, 4.0- and 3.4-fold, respectively, as compared with those in the SR RAA, and the relative *P311* mRNA in the AF RAA was significantly downregulated by 5.6-fold compared with the SR RAA. Therefore, the trend of mRNA expression changes as determined by real-time RT-PCR was in good agreement with that determined by the AF Chip (Fig. 3).

Fig. 4 shows the comparisons of relative mRNA expression determined by real time RT-PCR of the four selected genes in the LAA and RAA of AF subjects. Expression of *FHL1*, *TSC-22* and *CARP* was significantly increased, and the levels were similar in the right and left atria during AF. Interestingly, the fold decrease in *P311* mRNA expression in the LAA with AF was approximately twice that of *P311* mRNA expression in the RAA.

3.4 Increased distributions of FHL1 and CARP in the atria with AF

To determine whether the increased *FHL1* and *CARP* mRNA levels also resulted in an increase in protein levels in pacing-induced AF atria, we performed a western blotting analysis. As shown in Fig. 5, a 2.9-fold and 1.6-fold average increase in FHL1 and CARP, respectively, was observed in the fibrillating atria. These FHL1 and CARP protein expression data are consistent with the mRNA expression data of the cDNA array and quantitative real-time RT-PCR.

For confirming the increased expression of both FHL1 and CARP in rapid-pacing induced AF upon quantitative real-time RT-PCR and Western blot analysis, we investigated the intracellular distribution of FHL1 and CARP in porcine atrial appendage tissue with SR and AF using immunohistochemical assay (Fig. 6). By the immunohistochemical assay, FHL1 and CARP proteins were detectable in almost all myofibrils in atrial myocytes and increased positive immunoreaction coincides with muscle striated and filamentous forms in the atrial myocytes in AF. Furthermore, the both of anti-FHL1 and -CARP antibodies detected more diffuse cytoplasmic staining with slightly increased nuclear localization in the fibrillating atria (Fig. 6B and 6D).

3.5 Histological findings in the rapid-pacing induced AF

Histological studies were performed to identify the potential pathological substrate underlying conduction abnormalities in the sustained AF. Representatively histological sections from the atria with AF and SR were stained with Hematoxylin-eosin and Masson's trichrome blue. Evidences provided by the Masson's trichrome blue showed that endocardial fibrosis and extracellular matrix proteins markedly accumulated in

interstices between cardiomyocytes in the AF atria (Fig. 7).

3.6 Selective increase of TGF-β isoform expression in the fibrillating atria

Because increased expression of *TSC-22* gene and decreased expression of *P311* gene in atrium with AF may be associated with increased TGF-β signal activity, we examined levels of expression of *TGF-β* isoforms. By real-time RT-PCR analysis, expression of *TGF-β2* RNA levels were markedly increased 6.0-fold in RAA and 8.8-fold in LAA during AF, and *TGF-β1* mRNA were slightly increased respectively by 2.0-fold and 2.9-fold, however, *TGF-β3* mRNA levels were no significant change (Fig. 8). These results indicated that a selective increase of expression of *TGF-β1* and *-β2* isoforms was occurred in the pacing-induced AF.

3.7 Effects of Ang II, isoproterenol, and H_2O_2 on FHL1 and CARP mRNA expression in rat cardiac H9c2 cells

Several studies have indicated that the Ang II system, adrenergic signal transduction and oxidative stress are associated with the cellular signaling mechanisms in AF [6,18]. To determine whether proarrhythmogenic substrates alter the expression of *FHL1* or *CARP* in cardiac myocytes, H9c2 cells were treated with Ang II, the adrenergic agonist isoproterenol, or H_2O_2, and *FHL1* and *CARP* transcript levels were measured by semi-quantitative RT-PCR. The cells were pre-treated with differentiation-promoting medium (containing 1% FCS) for 48 h and then treated with 1 μM Ang II, 10 μM isoproterenol, or 200 μM H_2O_2 for 12 h. *FHL1* and *CARP* expression significantly increased 3.1- and 3.3-fold, respectively, in the H9c2 cells following treatment with isoproterenol, *CARP* expression slightly increased with Ang II treatment, but the two

genes expression did not increase in response to H_2O_2 (Fig. 9).

4. Discussion

AF is a progressive and self-sustaining disease. The processes include electrical, contractile, neurohormonal, macroanatomical and ultrastructural changes, and these may lead to the vulnerability of AF over time. Many factors such as ion channels, proteins influencing calcium homeostasis, connexins, autonomic innervation, fibrosis, and cytokines may be involved in the molecular mechanism of AF [1,2]. In the present study, a porcine model with sustained AF in which structural changes in the atrium [9,10] are induced by 4 weeks of rapid atrial depolarization was used to obtain more insight to molecular processes of atrial remodeling. Genes involved in transcriptional regulation, ion transport, signal transduction, metabolism, cell proliferation, extracellular matrix and structural proteins, and a few unclassified genes were used to study the differential expression in AF via a low-density cDNA array, named AF Chip (Fig. 1). To evaluate the threshold in differential expression of mRNA in our AF Chip, mock hybridization of two differentially labeled cDNAs to three replicates was first performed. More than 98% of the visible signals revealed Cy5/Cy3 ratios between 0.67 and 1.50 (data not shown). These ratios were used as cut-off values to identify significant differential expression throughout our experiments, in addition, the consistent and reliable AF Chip processes were also confirmed (Fig. 2). Results from the AF Chip analysis revealed that 31 mRNAs out of 84 clones were differentially expressed in atrial tissues (ratios ≥ 1.50 or ≤ 0.67; $P < 0.05$) in the rapid pacing-induced AF model (Table 2). Most observation of the 31 genes included those involved in

406 activation of signal transduction systems, transcriptional regulation and structural
407 alterations characteristic of AF. These alterations in expression by AF Chip assay might
408 be the focal or varied changes within the atrial tissue induced by AF, however, a locally
409 pronounced change might affect whole atrial function gradually like as an
410 arrhythmogenic substrate in AF.

411 Confirmatory real-time RT-PCR supported our AF Chip findings and emphasized
412 the marked differential expression of the transcriptional regulator genes *FHL1*, *CARP*
413 and *TSC-22* and an anti-fibrotic gene, *P311*, in the LAA and RAA tissues with AF (Fig.
414 3 and 4). Furthermore, FHL1 and CARP protein levels were also confirmed by western
415 blotting (Fig. 5).

416 The LIM domain of FHL1 is located at the amino terminus, which is associated
417 with GATA1-type zinc fingers [19], and the role of FHL1 in transcriptional regulation
418 was proposed [16]. Besides the function in transcriptional regulation, FHL1 has also
419 shown integrin-dependent localization in the nucleus, cytoskeleton, focal adhesions and
420 stress fibers in cardiomyocytes [20]. The CARP protein, a nuclear transcriptional co-
421 factor that negatively regulates cardiac gene expression [15], was upregulated in human
422 heart failure and animal models of cardiac hypertrophy [21,22]. Witt et al. [23]
423 demonstrated that CARP variably localizes in the sarcoplasm and the nucleus in adult
424 skeletal muscle cells. There was documented that CARP overexpression induces
425 contractile dysfunction in an engineered heart tissue [24].

426 Upon the information of molecular functions for FHL1 and CARP, they are
427 proposed as the critical roles in the transcriptional regulation, myofibrillar assembly and
428 even communication between sarcoplasm and nucleus in the cardiomyocytes [20,24].
429 In the present study, increased expressions and distributions of FHL1 and CARP in AF

atrial myocytes were detected, revealing that they may play a role associated partially with structures of the striated sarcomeres and protein filaments in AF atrial myofibrils (Fig. 6). Together these functional studies, the increased distributions of FHL1 and CARP might effect on atrial gene expression or contractility in the fibrillating atria by modulating transcription and myofilament assembly.

Factors that may contribute to progressive stability of AF with changed cellular signaling in a prolonged time course, also termed "arrhythmogenic substrates", have been discussed [18]. Among which, abnormal neurohormonal stimuli, such as angiotensin II (Ang II) and norepinephrine, may play a critical role in the sustained AF. Recent reports demonstrated activation of the renin angiotensin system (RAS) and RAS-dependent signaling pathways by AF in atria in humans [25] and in a dog model [26]. Ang II is an important modulator of cardiac and cardiomyocyte contractility. Ang II has been shown to exacerbate contractile dysfunction in experimental models of pressure-overload cardiac hypertrophy [27] and pacing- or infarction-induced heart failure [28,29]. In addition to RAS, sympathetic hyperinnervation, nerve sprouting, and a heterogeneous increase in atrial sympathetic stimulation have also been demonstrated in a canine model of sustained AF produced by prolonged right atrial pacing [30]. By isoproterenol infusion, Doshi et al. [31] demonstrated that the rapid automatic activity trigger the onset of AF, which occurs only in the atrium harvested from dogs with long-term pacing-induced AF but not in normal atrium. These findings underline the well-known profibrillatory effect resulting from a local excess of catecholamines [32]. The most important pattern of signal transduction linking the sympathetic nervous system to the intracellular effector in cardiomyocytes is mediated through the β1- and β2-adrenoceptors. The β-adrenergic receptors are stimulated by the catecholamines, which

initiates a cascade of intracellular events that leads to an increase in conduction velocity and shortening of the refractory period.

Direct effect of oxidative stress on atrial remodeling in a pacing-induced AF was also demonstrated by Carnes et al. [33]. Mihm et al. [34] found that increased oxidative stress during AF could contribute to contractile dysfunction. Most effects of mentioned above, neurohormonal stimuli and oxidative stress, can be provoked by the rapid atrial pacing and appear to be of importance for molecular changes in fibrillating atrium and effect on atrial contractile dysfunction [26,30,33].

We speculated that the FHL1 and CARP expression may be affected by neurohormonal stimuli and/or oxidative stress, since the two proteins represent the roles as the transcription regulators, myofilament components and were upregulated in this AF mode with rapid atrial depolarization for 6 weeks. Therefore, we were undertaken to investigate whether the expressions of *FHL1* and *CARP* in cardiomyocytes *in vitro* are directly regulated due to these proarrhythmogenic stimulations which were implicated in the atrial remodeling during AF. We found that the β-adrenergic agonist isoproterenol, but not Ang II or H_2O_2, significantly increased mRNA expression of both *FHL1* and *CARP* in H9c2 cells (Fig. 9). The rapid upregulation of *FHL1* and *CARP* expression in H9c2 cells stimulated by isoproterenol showed that regulation of the two genes may be mediated via the βAR signal transduction pathway. In the fibrillating atria, there was also evidence that the upregulated *β_2AR* mRNA was observed by cDNA array analysis (Table 2); these results implicate that upregulation of *FHL1* and *CARP* in the fibrillating atria might be associated with the activation of βAR signal pathway. In the study performed by Gaussin et al. [35], the expression of *FHL1* was dramatically upregulated in different mouse models of overexpressing β_1AR, β_2AR or PKA,

indicating that *FHL1* expression is upregulated by the βAR-PKA pathway. In addition, induced expression of CARP in cardiomyocytes by activation of PKA and CaMK was also obtained [24]. These studies strongly support our suggestions that the βAR signal pathway might be activated to upregulate two important regulators, *FHL1* and *CARP*, and effect on the changes of transcriptional regulation and atrial contractile in AF.

The increased expression of *CARP* induced by Ang II in H9c2 cells has also been detected (Fig. 9B). Ang II affects the expression of a wide range of signaling pathways [6]. Therefore, we would not exclude the possibility that upregulated expression of *CARP* in the pacing-induced AF model might be partially effected by activation of RAS signal pathway. However, the results of the *in vitro* experiment demonstrate that *FHL1* and *CARP* expression were not elevated in the H_2O_2-treated H9c2 cells, suggesting that changes in *FHL1* and *CARP* expression may be not associated with modulation of gene expression via oxidative damage in the fibrillating atria. These results of *in vitro* experiments provide a reference value to ongoing studies of the underlying molecular mechanism and even for novel insight in strategy of AF treatment. Nevertheless, with only limited studies in cardiac H9c2 cells in this regard, the results of changed *FHL1* and *CARP* expressions associated with cell signaling and transcription regulation in AF may be fundamental and deserve future investigations.

Calcium overload in AF was suggested a critical factor in the electrophysiological remodeling process and altered contraction and signaling in cardiomyocytes [36,37]. It is commonly believed that even minutes of rapid atrial rates can result in intracellular calcium overload, which decreases the L-type calcium current (I_{CaL}) [38]. In the present study, the mRNA expression levels of genes for L-type voltage-dependent calcium channel alpha-1C and-1S subunits (CACNA1C and CACNA1S), involved in

influencing calcium homeostasis, were also evaluated in our microarray analysis (Fig. 1). However, no significantly different was found between the AF and sham control groups. Our results seem to disagree with the published literature suggesting a decrease in L-type Ca^{2+} channel density that contributes to the reduction of I_{CaL} [36]. Nevertheless, studies on gene expression of the L-type Ca^{2+} channel, so far, have reported different results in AF. Schotten et al. [39] reported that there is no change in L-type Ca^{2+} channel density in persistent AF patients. An ultrastructural calcium distribution in goat atria with 1–16 weeks of burst-pacing-induced AF was performed [40]. Ausma et al. [40] showed that Ca^{2+} overload persists for 2 weeks, after which the cardiomyocytes apparently adapt to a new Ca^{2+} homeostasis and reach normal level, and then Ca^{2+} levels are below normal level after 16 weeks of AF. This study implicated that Ca^{2+} overload induced by over-drive pacing is reversible. Accordingly, we conceived that the new Ca^{2+} homeostasis and even recovery expression of calcium channel might be taken place in our AF model, which was induced by atrial rapid pacing for 4 weeks and then maintained AF without pacing for 2 weeks. Although the clear mechanism of reversible downregulation of I_{CaL} has not yet been uncovered, the calcium channel expression might be unchanged or have be recovery in our pacing-induced AF and play in part roles for the new Ca^{2+} homeostasis. Interestingly, the mRNA expression of calmodulin 2 (*CALM 2*) was increased by 1.7-fold in our AF model (Table 2). CALM is a critical Ca^{2+} sensor and regulatory protein and the formation of Ca^{2+}/ CALM complex selectively activates specific downstream signaling pathways in response to local changes in calcium concentration [41]. We suggest that the increased CALM 2 in AF might act as a critical Ca^{2+} sensor for the modulatory effects on calcium channels function or downstream signaling and therefore to

526 overcome the detrimental Ca^{2+} overload. However, much additional work in this
527 regard, such as the respective roles of functional (Na^+, K^+, Ca^{2+}, and Cl^-) channels and
528 the precise signaling of Ca^{2+}/CaML, need to be performed to truly understand the
529 changes and effects of Ca^{2+} homeostasis in AF.

530 A number of cardiovascular diseases are associated with extracellular matrix
531 homeostasis [42,43]. The occurrence of atrial fibrosis in the development of AF has
532 been documented [44-46] and also found in our AF model (Fig. 7). Interesting, an
533 unclassified gene, *P311*, was markedly downregulated in the fibrillating atria. Recent
534 studies indicate that P311 blocks TGF-β autoinduction and downregulates the
535 expression of genes encoding extracellular matrix proteins in cardiac myofibroblasts,
536 suggesting that P311 exerts anti-fibrotic effects by inhibiting TGF-β signaling [47].
537 Furthermore, TSC-22 is a TGF-β-inducible gene and represent a transcriptional
538 regulator that enhances the activity of TGF-β signaling by binding to and modulating
539 the transcriptional activity of Smad3 and Smad4 [48]. The expression of *TSC-22* was
540 significantly induced by 4.0-fold in our AF model, implicating the enhanced activation
541 of TGF-β signaling in the fibrillating atria. In concordance with our supposition, we
542 identified the upregulated expressions of *TGF-β* isoforms in the AF model by real-time
543 RT-PCR analysis. The expression of *TGF-β2* RNA levels were markedly increased in
544 atrial tissues with AF and *TGF-β1* RNA were slightly increased; however, *TGF-β3*
545 RNA levels were no significant change (Fig. 8). Interestingly, the differently
546 upregulated levels of *TGF-β2* between RAA and LAA with AF seemingly showed the
547 parallel with the decreased expression of *P311* in atrial tissues (Fig. 4 and 8),
548 implicating that effects of *TGF-β2* expression in AF may at least partially result from

549 loss of P311 blocked TGF-β autoinduction. Recent studies have demonstrated an
550 upregulation of *TGF-β1* expression in human AF patients by microarray analysis,
551 indicating activation of *TGF-β1* signaling is involved in the process of development
552 fibrosis in AF [3,4]. Beside, the studies on transgenic mice have also shown that
553 increased cardiac expression of TGF-β1 leads to atrial fibrosis [49] and increased
554 vulnerability to AF [50]. The upregulation of *TGF-β1* and *-β2* identified in the rapid-
555 pacing induced AF model may therefore promote the activation of fibroblasts and atrial
556 fibrosis. These results suggest that the dramatic *P311* downregulation and *TSC-22*
557 upregulation may play a significant critical role and contribute to the development of
558 fibrosis during AF while the increased *TGF-β1* and *-β2* expression were also obtained.

559 In conclusion, use of a low-density cDNA array of 84 selected genes identified
560 four genes, *FHL1*, *CARP*, *TSC-22* and *P311*, as differentially expressed in the rapid-
561 pacing induced AF model in pig. The observed alterations in AF were proven by further
562 identification of protein expression and possible mechanism in the fibrillating atria.
563 These data implicated that the changes in transcriptional regulator expressions,
564 myofilament assembly and genes responsible for TGF-β signaling might play a
565 significant functional role in AF-induced the structural alterations, such as atrial
566 contractile dysfunction and interstitial fibrosis, and provide future avenues for
567 investigation of the underlying mechanisms of AF pathogenesis.

568

569 **Acknowledgments**

570 This work was supported by the grants of NSC 92-2314-B-009-001-B32 and NSC

93-2314-B-009-001-B32 from the National Science Council and the grants of VGHUST93-G5-05-4 and VGHUST94-G5-05-4 from the Veterans General Hospitals, University System of Taiwan, Taiwan.

References

[1] M. Allessie, J. Ausma, U. Schotten, Electrical, contractile and structural remodeling during atrial fibrillation, Cardiovasc. Res. 54 (2002) 230-246.

[2] S. Levy, P. Sbragia, Remodelling in atrial fibrillation, Arch. Mal. Coeur. Vaiss. 98 (2005) 308-312.

[3] A.S. Barth, S. Merk, E. Arnoldi, L. Zwermann, P. Kloos, M. Gebauer, K. Steinmeyer, M. Bleich, S. Kaab, M. Hinterseer, H. Kartmann, E. Kreuzer, M. Dugas, G. Steinbeck, M. Nabauer, Reprogramming of the human atrial transcriptome in permanent atrial fibrillation: expression of a ventricular-like genomic signature, Circ. Res. 96 (2005) 1022-1029.

[4] G. Lamirault, N. Gaborit, N. Le Meur, C. Chevalier, G. Lande, S. Demolombe, D. Escande, S. Nattel, J.J. Leger, and M. Steenman, Gene expression profile associated with chronic atrial fibrillation and underlying valvular heart disease in man, J. Mol. Cell. Cardiol. 40 (2006) 173-184.

[5] N.H. Kim, Y. Ahn, S.K. Oh, J.K. Cho, H.W. Park, Y.S. Kim, M.H. Hong, K.I. Nam, W.J. Park, M.H. Jeong, B.H. Ahn, J.B. Choi, H. Kook, J.C. Park, J.W. Jeong, J.C. Kang, Altered patterns of gene expression in response to chronic atrial fibrillation, Int. Heart J. 46 (2005) 383-395.

[6] A. Goette, U. Lendeckel, H.U. Klein, Signal transduction systems and atrial fibrillation, Cardiovasc. Res. 54 (2002) 247-258.

[7] M.A. Allessie, P.A. Boyden, A.J. Camm, A.G. Kleber, M.J. Lab, M.J. Legato, M.R. Rosen, P.J. Schwartz, P.M. Spooner, D.R. Van Wagoner, and A.L. Waldo, Pathophysiology and prevention of atrial fibrillation, Circulation 103 (2001) 769-

777.

[8] S. Nattel, A. Shiroshita-Takeshita, B.J. Brundel, L. Rivard, Mechanisms of atrial fibrillation: lessons from animal models, Prog. Cardiovasc. Dis. 48 (2005) 9-28.

[9] J.L. Lin, L.P. Lai, C.S. Lin, C.C. Du, T.J. Wu, S.P. Chen, W.C. Lee, P.C. Yang, Y.Z. Tseng, W.P. Lien, S.K. Huang, Electrophysiological mapping and histological examinations of the swine atrium with sustained (> or =24 h) atrial fibrillation: a suitable animal model for studying human atrial fibrillation, Cardiology 99 (2003) 78-84.

[10] L.P. Lai, J.L. Lin, C.S. Lin, H.M. Yeh, Y.G. Tsay, C.F. Lee, H.H. Lee, Z.F. Chang, J.J. Hwang, M.J. Su, Y.Z. Tseng, S.K. Huang, Functional genomic study on atrial fibrillation using cDNA microarray and two-dimensional protein electrophoresis techniques and identification of the myosin regulatory light chain isoform reprogramming in atrial fibrillation, J. Cardiovasc. Electrophysiol. 15 (2004) 214-223.

[11] C.S. Lin, C.W. Hsu, Differentially transcribed genes in skeletal muscle of Duroc and Taoyuan pigs, J. Anim. Sci. 83 (2005) 2075-2086.

[12] B.J. Brundel, I.C. Van Gelder, R.H. Henning, R.G. Tieleman, A.E. Tuinenburg, M. Wietses, J.G. Grandjean, W.H. Van Gilst, H.J. Crijns, Ion channel remodeling is related to intraoperative atrial effective refractory periods in patients with paroxysmal and persistent atrial fibrillation, Circulation 103 (2001) 684-690.

[13] K.J. Livak, T.D. Schmittgen, Analysis of relative gene expression data using real-time quantitative PCR and the 2(-Delta Delta C(T)) Method, Methods 25 (2001) 402-408.

[14] Y. Takagi, R.C. Conaway, J.W. Conaway, Characterization of elongin C functional

621 domains required for interaction with elongin B and activation of elongin A, J.
622 Biol. Chem. 271 (1996) 25562-25568.
623 [15] Y. Zou, S. Evans, J. Chen, H.C. Kuo, R.P. Harvey, K.R. Chien, CARP, a cardiac
624 ankyrin repeat protein, is downstream in the Nkx2-5 homeobox gene pathway,
625 Development 124 (1997) 793-804.
626 [16] Y. Taniguchi, T. Furukawa, T. Tun, H. Han, T. Honjo, LIM protein KyoT2
627 negatively regulates transcription by association with the RBP-J DNA-binding
628 protein, Mol. Cell. Biol. 18 (1998) 644-654.
629 [17] S. Hino, H. Kawamata, D. Uchida, F. Omotehara, Y. Miwa, N.M. Begum, H.
630 Yoshida, T. Fujimori, M. Sato, Nuclear translocation of TSC-22 (TGF-beta-
631 stimulated clone-22) concomitant with apoptosis: TSC-22 as a putative
632 transcriptional regulator, Biochem. Biophys. Res. Commun. 278 (2000) 659-664.
633 [18] A. Goette, U. Lendeckel, Nonchannel drug targets in atrial fibrillation, Pharmacol.
634 Ther. 102 (2004) 17-36.
635 [19] M.J. Morgan, A.J. Madgwick, Slim defines a novel family of LIM-proteins
636 expressed in skeletal muscle, Biochem. Biophys. Res. Commun. 225 (1996) 632-
637 638.
638 [20] P.A. Robinson, S. Brown, M.J. McGrath, I.D. Coghill, R. Gurung, C.A. Mitchell,
639 Skeletal muscle LIM protein 1 regulates integrin-mediated myoblast adhesion,
640 spreading, and migration, Am. J. Physiol. Cell Physiol. 284 (2003) 681-695.
641 [21] O. Zolk, M. Frohme, A. Maurer, F.W. Kluxen, B. Hentsch, D. Zubakov, J.D.
642 Hoheisel, I.H. Zucker, S. Pepe, T. Eschenhagen, Cardiac ankyrin repeat protein, a
643 negative regulator of cardiac gene expression, is augmented in human heart failure,
644 Biochem. Biophys. Res. Commun. 293 (2002) 1377-1382.

645 [22] Y. Aihara, M. Kurabayashi, Y. Saito, Y. Ohyama, T. Tanaka, S. Takeda, K. Tomaru,
646 K. Sekiguchi, M. Arai, T. Nakamura, R. Nagai, Cardiac ankyrin repeat protein is a
647 novel marker of cardiac hypertrophy: role of M-CAT element within the promoter,
648 Hypertension 36 (2000) 48-53.
649 [23] C.C. Witt, Y. Ono, E. Puschmann, M. McNabb, Y. Wu, M. Gotthardt, S.H. Witt, M.
650 Haak, D. Labeit, C.C. Gregorio, H. Sorimachi, H. Granzier, S. Labeit, Induction
651 and myofibrillar targeting of CARP, and suppression of the Nkx2.5 pathway in the
652 MDM mouse with impaired titin-based signaling, J. Mol. Biol. 336 (2004) 145-
653 154.
654 [24] O. Zolk, M. Marx, E. Jackel, A. El-Armouche, T. Eschenhagen, Beta-adrenergic
655 stimulation induces cardiac ankyrin repeat protein expression: involvement of
656 protein kinase A and calmodulin-dependent kinase, Cardiovasc. Res. 59 (2003)
657 563-572.
658 [25] A. Goette, T. Staack, C. Rocken, M. Arndt, J.C. Geller, C. Huth, S. Ansorge, H.U.
659 Klein, U. Lendeckel, Increased expression of extracellular signal-regulated kinase
660 and angiotensin-converting enzyme in human atria during atrial fibrillation, J. Am.
661 Coll. Cardiol. 35 (2000) 1669–1677.
662 [26] D. Li, K. Shinagawa, L. Pang, T.K. Leung, S. Cardin, Z. Wang, S. Nattel, Effects of
663 angiotensin-converting enzyme inhibition on the development of the atrial
664 fibrillation substrate in dogs with ventricular tachypacing-induced congestive heart
665 failure, Circulation 104 (2001) 2608–2614.
666 [27] A. Meissner, J.Y. Min, R. Simon, Effects of angiotensin II on inotropy and
667 intracellular Ca2+ handling in normal and hypertrophied rat myocardium, J. Mol.
668 Cell. Cardiol. 30 (1998) 2507-2518.

669 [28] C.P. Cheng, M. Suzuki, N. Ohte, M. Ohno, Z.M. Wang, W.C. Little, Altered
670 ventricular and myocyte response to angiotensin II in pacing-induced heart failure,
671 Circ. Res. 78 (1996) 880-892.
672 [29] J.M. Capasso, P. Li, X. Zhang, L.G. Meggs, P. Anversa, Alterations in ANG II
673 responsiveness in left and right myocardium after infarction-induced heart failure
674 in rats, Am. J. Physiol. 264 (1993) 2056-2067.
675 [30] J.V. Jayachandran, H.J. Sih, W. Winkle, D.P. Zipes, G.D. Hutchins, J.E. Olgin,
676 Atrial fibrillation produced by prolonged rapid atrial pacing is associated with
677 heterogeneous changes in atrial sympathetic innervation, Circulation 101 (2000)
678 1185-1191.
679 [31] R.N. Doshi, T.J. Wu, M. Yashima, Y.H. Kim, J.J. Ong, J.M. Cao, C. Hwang, P.
680 Yashar, M.C. Fishbein, H.S. Karagueuzian, P.S. Chen, Relation between ligament
681 of Marshall and adrenergic atrial tachyarrhythmia, Circulation 100 (1999) 876-883.
682 [32] C.M. Chang, T.J. Wu, S. Zhou, R.N. Doshi, M.H. Lee, T. Ohara, M.C. Fishbein,
683 H.S. Karagueuzian, P.S. Chen, L.S. Chen, Nerve sprouting and sympathetic
684 hyperinnervation in a canine model of atrial fibrillation produced by prolonged
685 right atrial pacing, Circulation 103 (2001) 22-25.
686 [33] C.A. Carnes, M.K. Chung, T. Nakayama, H. Nakayama, R.S. Baliga, S. Piao, A.
687 Kanderian, S. Pavia, R.L. Hamlin, P.M. McCarthy, J.A. Bauer, D.R. Van Wagoner,
688 Ascorbate attenuates atrial pacing-induced peroxynitrite formation and electrical
689 remodeling and decreases the incidence of postoperative atrial fibrillation, Circ.
690 Res. 89 (2001) 32-38.
691 [34] M.J. Mihm, F. Yu, C.A. Carnes, P.J. Reiser, P.M. McCarthy, D.R. Van Wagoner,
692 J.A. Bauer, Impaired myofibrillar energetics and oxidative injury during human

693 atrial fibrillation, Circulation 104 (2001) 174-180.
694 [35] V. Gaussin, J.E. Tomlinson, C. Depre, S. Engelhardt, C.L. Antos, G. Takagi, L.
695 Hein, J.N. Topper, S.B. Liggett, E.N. Olson, M.J. Lohse, S.F. Vatner, D.E. Vatner,
696 Common genomic response in different mouse models of beta-adrenergic-induced
697 cardiomyopathy, Circulation 108 (2003) 2926-2933.
698 [36] S. Nattel, Atrial electrophysiological remodeling caused by rapid atrial activation:
699 underlying mechanisms and clinical relevance to atrial fibrillation, Cardiovasc. Res.
700 42 (1999) 298-308.
701 [37] H. Sun, D. Chartier, N. Leblanc, S. Nattel, Intracellular calcium changes and
702 tachycardia-induced contractile dysfunction in canine atrial myocytes, Cardiovasc.
703 Res. 49 (2001) 751-761.
704 [38] C. Pandozi, M. Santini, Update on atrial remodelling owing to rate; does atrial
705 fibrillation always 'beget' atrial fibrillation? Eur. Heart J. 22 (2001) 541-553.
706 [39] U. Schotten, H. Haase, D. Frechen, M. Greiser, C. Stellbrink, J.F. Vazquez-
707 Jimenez, I. Morano, M.A. Allessie, P. Hanrath, The L-type Ca^{2+}-channel subunits
708 alpha1C and beta2 are not downregulated in atrial myocardium of patients with
709 chronic atrial fibrillation, J. Mol. Cell. Cardiol. 35 (2003) 437-443.
710 [40] J. Ausma, G.D. Dispersyn, H. Duimel, F. Thone, L. Ver Donck, M.A. Allessie, M.
711 Borgers, Changes in ultrastructural calcium distribution in goat atria during atrial
712 fibrillation, J. Mol. Cell. Cardiol. 32 (2000) 355-364.
713 [41] N. Frey, T.A. McKinsey, E.N. Olson, Decoding calcium signals involved in cardiac
714 growth and function, Nat. Med. 6 (2000) 1221-1227.
715 [42] F.G. Spinale, Matrix metalloproteinases: regulation and dysregulation in the failing
716 heart, Circ. Res. 90 (2002) 520-530.

717 [43] C.M. Dollery, J.R. McEwan, A.M. Henney, Matrix metalloproteinases and
718 cardiovascular disease, Circ. Res. 77 (1995) 863-868.
719 [44] H. Hayashi, C. Wang, Y. Miyauchi, C. Omichi, H.N. Pak, S. Zhou, T. Ohara, W.J.
720 Mandel, S.F. Lin, M.C. Fishbein, P.S. Chen, H.S. Karagueuzian, Aging-related
721 increase to inducible atrial fibrillation in the rat model, J. Cardiovasc.
722 Electrophysiol. 13 (2002) 801-808.
723 [45] C. Boixel, V. Fontaine, C. Rucker-Martin, P. Milliez, L. Louedec, J.B. Michel, M.P.
724 Jacob, S.N. Hatem, Fibrosis of the left atria during progression of heart failure is
725 associated with increased matrix metalloproteinases in the rat, J. Am. Coll. Cardiol.
726 42 (2003) 336-344.
727 [46] M. Sakabe, A. Fujiki, K. Nishida, M. Sugao, H. Nagasawa, T. Tsuneda, K.
728 Mizumaki, H. Inoue, Enalapril prevents perpetuation of atrial fibrillation by
729 suppressing atrial fibrosis and over-expression of connexin43 in a canine model of
730 atrial pacing-induced left ventricular dysfunction, J. Cardiovasc. Pharmacol. 43
731 (2004) 851-859.
732 [47] S. Paliwal, J. Shi, U. Dhru, Y. Zhou, L. Schuger, P311 binds to the latency
733 associated protein and downregulates the expression of TGF-beta1 and TGF-beta2,
734 Biochem. Biophys. Res. Commun. 315 (2004) 1104-1109.
735 [48] S.J. Choi, J.H. Moon, Y.W. Ahn, J.H. Ahn, D.U. Kim, T.H. Han, Tsc-22 enhances
736 TGF-beta signaling by associating with Smad4 and induces erythroid cell
737 differentiation, Mol. Cell. Biochem. 271 (2005) 23-28.
738 [49] H. Nakajima, H.O. Nakajima, O. Salcher, A.S. Dittie, K. Dembowsky, S. Jing, L.J.
739 Field, Atrial but not ventricular fibrosis in mice expressing a mutant transforming
740 growth factor-beta(1) transgene in the heart, Circ. Res. 86 (2000) 571-579.

741 [50] S. Verheule, T. Sato, T.t. Everett, S.K. Engle, D. Otten, M. Rubart-von der Lohe,
742 H.O. Nakajima, H. Nakajima, L.J. Field, J.E. Olgin, Increased vulnerability to atrial
743 fibrillation in transgenic mice with selective atrial fibrosis caused by
744 overexpression of TGF-beta1, Circ. Res. 94 (2004) 1458-1465.

745

746 **Figure legends**

747

748 Fig. 1. Design of the AF Chip. The 84 selected cDNA clones are members of the
749 following functional classes: extracellular matrix, structural components, signal
750 transduction, metabolism, ion transporters, cell proliferation, transcription regulation,
751 EST sequences, and others. Two housekeeping genes, β-tubulin and *GAPDH*, were
752 spotted onto the slides for signal normalization and positive controls. To evaluate the
753 reliability of the experimental hybridization, a blank and a negative control (pUC19)
754 were also included in the chip.

755

756 Fig. 2. Quality assessment of the AF Chip. A representative result from the AF Chip is
757 shown (A). AF Chip hybridization comparing mRNA isolated from AF and SR
758 (control) subjects. Message RNA from SR tissue was used to prepare cDNA labeled
759 with Cy3, and mRNA extracted from AF tissue was used to prepare cDNA labeled with
760 Cy5. The two cDNA probes were mixed and simultaneously hybridized to the AF Chip.
761 Red indicates genes whose mRNAs were more abundant in AF, and green indicates
762 genes whose mRNAs were more abundant in SR. Yellow spots represent genes whose
763 expression did not vary substantially between the two samples. Scatter-plot analyses of
764 spot intensities between duplicate spots with the Cy5 (B) and Cy3 (C) channels.

765

766 Fig. 3. Verification of altered gene expression by quantitative real-time RT-PCR.
767 Comparison of results obtained with the AF Chip and quantitative real-time RT-PCR for
768 mRNA levels of *FHL1*, *TSC-22*, *CARP* and *P311* during AF. Real-time RT-PCR and AF

769 Chip hybridizations were performed as described in the Materials and methods.
770 Relative to the levels in the RAA with SR, expression of *FHL1*, *TSC-22* and *CARP*
771 mRNAs was increased by 5.1-, 4.0- and 3.4-fold, respectively, in the parallel AF
772 subjects. *P311* mRNA expression was decreased by 5.6-fold in AF. Bar graphs with
773 error bars represent the means ± SD (n = 12 for real-time RT-PCR and chip analysis).

774

775 Fig. 4. Comparisons of mRNA expression in the RAA and LAA with AF. The cDNAs
776 were prepared from the RAA and LAA of AF and SR groups and then subjected to real-
777 time PCR with gene-specific primers. The ratio of the abundance of each transcript to
778 that of the *GAPDH* transcript was calculated, and the amount of mRNA expression in
779 the AF group was expressed as a relative change standardized to the control group. Bar
780 graphs with error bars represent the means ± SD (n = 6 in the SR group; n = 12 in the
781 LAA and RAA of the AF group). **P* < 0.05 *vs.* RAA.

782

783 Fig. 5. Western blot analysis of FHL1 and CARP protein expression in SR and AF atria.
784 Tissue homogenates (20 μg protein/lane) from RAA with AF or SR were separated on
785 10% SDS-PAGE gels and transferred to polyvinylidene fluoride membrane.
786 Immunoblots were incubated with antibodies specific for FHL1, CARP or β-tubulin
787 (A). The relative protein expression of FHL1 (B) and CARP (C) was normalized to β-
788 tubulin. The histograms show the means ± SD (n = 6 in the SR group; n = 12 in the AF
789 group). **P* < 0.05 and ***P* < 0.01, *vs*. SR.

790

791 Fig. 6. Immunohistochemical assay of FHL1 and CARP protein in the atrial appendage

792 tissues with SR (A and C) and AF (B and D). Increased FHL1 and CARP are detectable
793 in almost all myofibrils in the atrial myocytes and positive immunoreaction coincides
794 with muscle striation and protein filaments in the muscle fibers in AF. In fibrillating
795 atria, immunostaining of FHL1 and CARP showed more abundant and disorganized (B
796 and D). (Scale bar represents 50 μm)

797

798 Fig. 7. Representative photomicrographs of atrial appendage tissue showing fibrosis in
799 rapid-pacing induced AF. Histological sections from the atrial appendage tissue with
800 SR (A) and AF (B) were stained by Masson's trichrome blue. The blue color
801 characteristic of collagen after Masson's trichrome staining was obvious in interstices
802 between cardiomyocytes in the AF atria. Sections from sham control, when stained
803 similarly reflect the extracellular matrix marked accumulation in the rapid-pacing
804 induced fibrillating atria. (Scale bar represents 100 μm)

805

806 Fig. 8. Three *TGF-β* isoforms mRNA levels in right and left atrial appendages with AF
807 compared with SR were determined by real-time RT-PCR. Differently expressed
808 changes of three *TGF-β* isoforms mRNA were observed in AF, and upregulation of
809 *TGF-β* 1 and -*β* 2 expression in RAA and LAA with AF were found. Expression of
810 *TGF-β2* mRNA levels were markedly increased 6.0-fold in RAA and 8.8-fold in LAA
811 during AF, and the changes of *TGF-β1* mRNA in RAA and LAA were increased
812 respectively by 2.0-fold and 2.9-fold, however, *TGF-β3* mRNA levels were no
813 significant change, when compared with SR. (n = 6 in the SR group; n = 12 in the AF
814 group). * $P < 0.05$ *vs*. SR, ** $P < 0.05$ *vs*. SR and † indicates $P < 0.05$ *vs.* RAA.

Fig. 9. Effects of Ang II, isoproterenol, or H_2O_2 on the transcription levels of *FHL1* and *CARP* in cardiac H9c2 cells. H9c2 cells grown to 80% confluency were treated with 1 μM Ang II, 10 μM isoproterenol (Isop), 200 μM H_2O_2 or PBS (as a control) for 12 h and then RNA was isolated for semi-quantitative RT-PCR. The fold changes in mRNA expression of *FHL1* (A) and *CARP* (B) were calculated based on *GAPDH* as a covariate. Data represent the means ± SD of three independent experiments. $*P < 0.05$, and $**P < 0.01$, *vs*. control.

837 **Table 1**

838 Primers for quantitative real-time RT-PCR.

839

Gene name (Gene symbol/Accession no.)	Primer [a]	Sequence (5' → 3')	Amplified length (bp)
Four and a half LIM domains 1 (FHL1/ NM_214375)	Forward	CTG CGT GGA TTG CTA CAA GA	115
	Reverse	GTG CCA GGA TTG TCC TTC AT	
Transforming growth factor beta-stimulated clone 22 (TSC-22/ NM_006022)	Forward	CCA TGA AGG TTG TTT TGC T	130
	Reverse	ACC TCC TCA GAC AGC CAA T	
Cardiac ankyrin repeat protein (CARP/ NM_213922)	Forward	CTT CCC GTA GGT AGC TCT TA	122
	Reverse	GCA ACA ATC ATC CCC TCT G	
Chromosome 5 open reading frame 13 (P311/ NM_004772)	Forward	GCG AGG TAG CTC TGA TGG A	123
	Reverse	GCC ACA CTG AAG ACA CAA GG	
Glyceraldehyde-3-phosphate dehydrogenase (GAPDH/AF017079)	Forward	AGA AGA CTG TGG ATG GCC C	110
	Reverse	ATG ACC TTG CCC ACA GCC T	
Transforming Growth Factor β1 (TGF β 1/ NM_214015)	Forward	GGC CGT ACT GGC TCT TTA CA	138
	Reverse	TAG ATT TGG TTG CCG CTT TC	
Transforming Growth Factor β2 (TGF β2/ L08375)	Forward	ATG GCA CCT CCA CAT ATA CCA	101
	Reverse	GGG CAA CAA CAT TAG CAG GA	
Transforming Growth Factor β3 (TGF β 3/ NM_214198)	Forward	AAG AAG GAA CAC AGC CCT CA	116
	Reverse	GCG GAA GCA GTA GTT GGT GT	

840 [a] Primer sequences for each target gene were selected to minimize the formation of self-

841 complementarity and hairpins using the software Primer Express (PE Applied

842 Biosystems).

843

844 **Table 2**

845 Genes with significantly altered expression in the right atrial appendages with sustained

846 AF as assayed by the AF Chip.

Accession no.	Function/Gene name	Symbol	Ratio (Cy5/Cy3)	SD	*P* value
	Transcription-related genes				
AA725097	Four and a half LIM domains 1	FHL1	3.17 ↑	1.27	0.001
NM_006022	Transforming growth factor TSC-22	TSC-22	3.09 ↑	1.71	0.011
AA521128	Transcription elongation factor B (SIII)	TCEB1	2.49 ↑	1.10	0.001
X83703	Cardiac ankyrin repeat protein	CARP	1.61 ↑	0.45	0.001
	Structural components and extracellular matrix-related genes				
S69022	Myosin regulatory light polypeptide 2	MYL2	4.35 ↑	1.70	0.001
BE388159	Cysteine and glycine-rich protein 1	CSRP1	2.57 ↑	1.81	0.012
AI809596	Spondin 1	SPON1	2.05 ↑	1.13	0.017
X02761	Fibronectin 1	FN1	1.94 ↑	0.72	0.001
M34064	Cadherin 2	CDH2	1.76 ↑	0.77	0.005
AA043347	A disintegrin and metalloprotease domain 10	ADAM10	1.50 ↑	0.77	0.044
AA451883	Cartilage associated protein	CRTAP	0.63 ↓	0.49	0.025
AI189375	Matrix metalloproteinase 11	MMP11	0.48 ↓	0.38	0.001
	Signal transduction-related genes				
D45887	Calmodulin 2	CALM2	1.71 ↑	0.66	0.004
U02390	Beta-2 adrenergic receptor	B2AR	1.64 ↑	0.73	0.030
AW157548	Insulin-like growth factor binding protein 5	IGFBP5	1.55 ↑	0.72	0.022
	Cell proliferation-related genes				
Y12084	Cysteine-rich, angiogenic inducer, 61	CYR61	1.50 ↑	0.53	0.007
XM_001393	Natural killer-enhancing factor A	PRDX1	0.63 ↓	0.35	0.006
	Metabolism-related genes				
NM_001825	Creatine kinase	CKMT2	1.59 ↑	0.65	0.009
AI494124	Selenoprotein P, plasma, 1	SEPP1	0.69 ↓	0.36	0.015
AI207602	Hemoglobin, gamma G	HBG2	0.57 ↓	0.46	0.008
AW249010	Heat shock 70kD protein 10	HSPA8	0.53 ↓	0.35	0.001
	Genes with other functions and EST sequences				
NM_004854	HNK-1 sulfotransferase	CHST10	2.08 ↑	1.10	0.008
AA375284	Poly (rC)-binding protein 2	PCBP2	1.64 ↑	0.49	0.001
AI275225	MAX-like bHLHZIP protein	MLX	0.64 ↓	0.19	0.000
Z48042	Membrane surface marker 1	M11S1	0.60 ↓	0.40	0.005
AI815757	Ribosomal protein L35	RPL35	0.48 ↓	0.38	0.001
NM_004772	Chromosome 5 open reading frame 13	P311	0.40 ↓	0.17	0.000
AA431300	EST6		2.24 ↑	1.28	0.009
N92589	EST4		2.12 ↑	1.42	0.019
N93201	EST5		2.00 ↑	1.35	0.033
AA195902	EST14		0.66 ↓	0.31	0.011

847

848 The signal intensities of the competitive hybridization were quantified with a two-

channel (Cy3 and Cy5) fluorescence scanner. Analysis of the fluorescence intensities and expression ratios were performed using GenePix Pro 4.1 software. Data represent the mean and SD of the Cy5/Cy3 intensity ratios (n = 12). Those signal intensities more than 2 SDs from the background intensity and greater than the negative sham control intensity were considered as acceptable signals. This table lists results for which the differential expression was ≥1.5-fold, which was considered as significant ($P < 0.05$).

	1	2	3	4	5	6	7	8	9	10	11	12
A	GAPDH AI986320	Blank	pUC19	TUBB BC029529	Blank	TNNT2 BE393657	AGRT1 NM_009585	CALM D45887	LYN AA939217	CALM D45887	CAP2 U02390	ARF4 AA307503
B	EST1 AA923015	EST2 R09547	EST3 N44535	EST4 N92589	EST5 N93201	EST6 AA431300	EST7 AI051950	EST8 AI090186	PRKAR1A AA015682	IGFBP5 AW157548	PTGER4 L28175	TNFSF10 BE350219
C	EST9 AI188760	EST10 AI261936	EST11 AI380932	EST12 AI479494	EST13 AW051824	EST14 AA195902	EST15 AA922329	EST16 AW772770	EDN1 NM_001955	β2AR M15169	ACE M26658	ACE M26658
D	CACNA1C AJ224873	CACNA1S AI417964	CACNA1S AI417964	KCNK3 AI193606	GJB3 AW276400	GJA1 X52947	HSPA8 AW249010	PRDX1 X67951	CCND1 M73554	STATS3 AJ012463	BTEB1 D31716	TSC-22 NM_006022
E	MMP11 AI189375	ADAM10 AA043347	ADAM15 U41767	FN1 X02761	CKMT2 NM_001825	UCHL1 AI928978	LPL NM_000237	CYR61 Y12084	CAPNS1 BE397929	ZNF177 U37263	CARP X83703	MITF Z29678
F	CDH2 M34064	CHST10 NM_004854	CLDN1 AI300819	SPON1 AI809596	YWHAZ BE315169	HBG2 AI207602	SEPP1 AI494124	PRDX1 X67951	FHL1 AA725097	GTF2E2 S67861	BAZ2B AB032255	TCEB1 AA521128
G	CRTAP AA451883	PLS3 NM_005032	SPTBN1 M96803	ACTR1A AL120727	SERPINB2 Y00630	PCBP2 AA375284	CAV1 AI878826	M11S1 Z48042	CYFIP2 AB032994	U5-116KD D21163	CSRP1 BE388159	RPL35 AI815757
H	ACTG1 BE314833	ACTN1 X15804	MYL2 S69022	TUBB BC029529	MMP2 BQ674774	CAST U38525	AHR AA844153	HUMGT 198A AI275225	C5orF13 NM_004772	GAPDH AI986320	Blank	pUC19

Positive and negative control
Blank
EST clones
Connexin and ion transporter related genes
Structural component and extracellular matrix related genes
Signal transduction related genes
Transcription related genes
Metabolism related genes
Cell proliferation related genes
Other genes

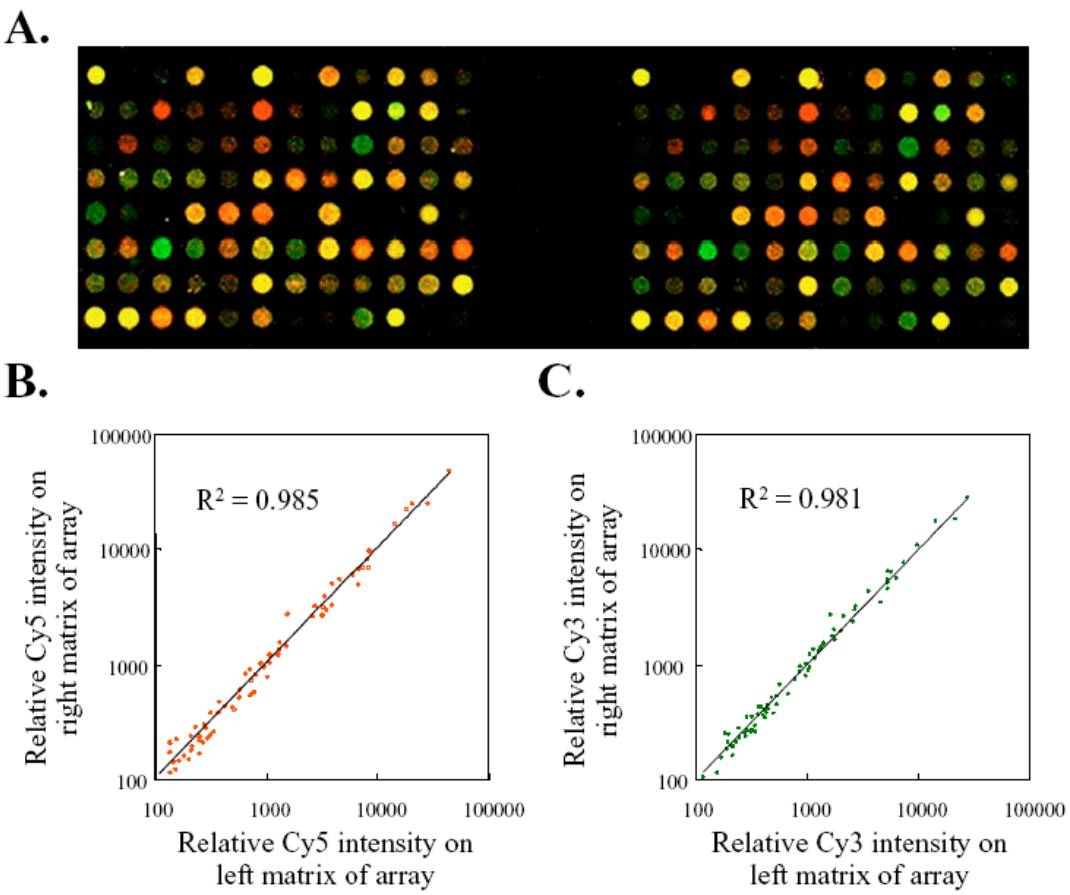

882

883

884

885

886

887

888

889

890

891

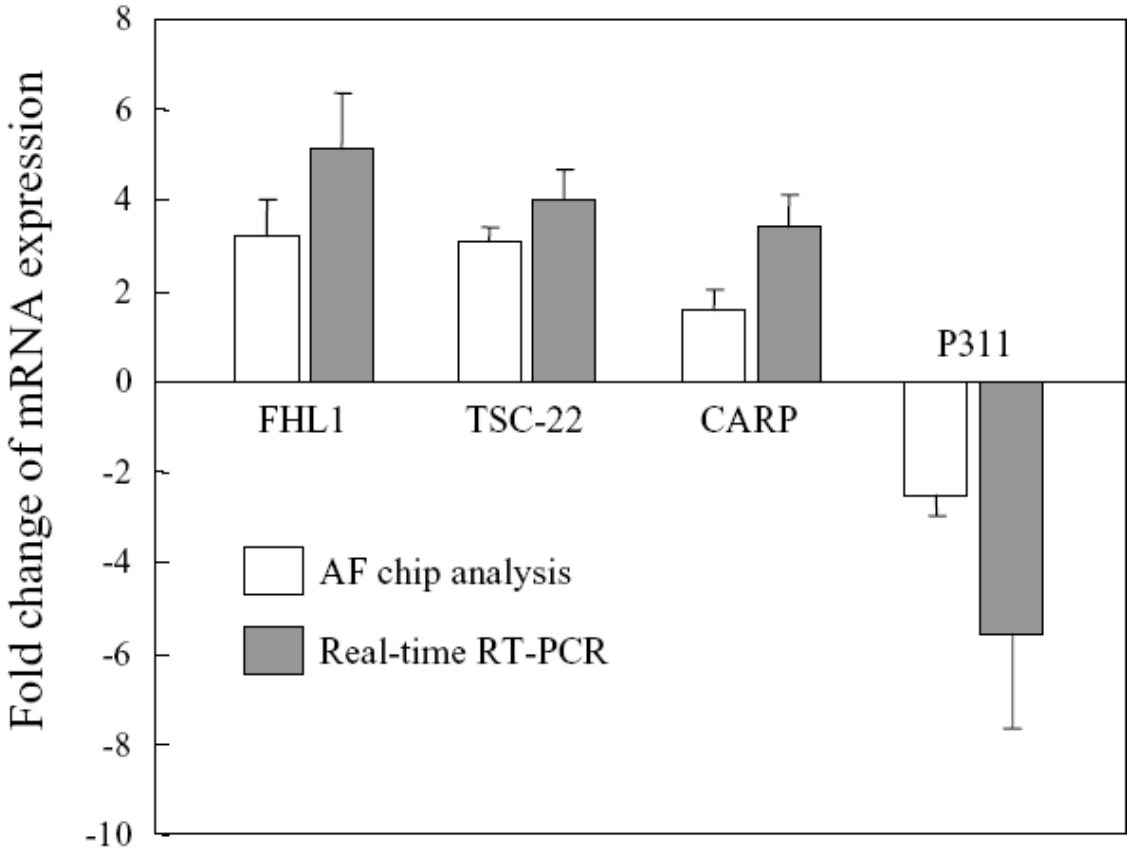

892

893

894

895

896

897

898

899

900

901

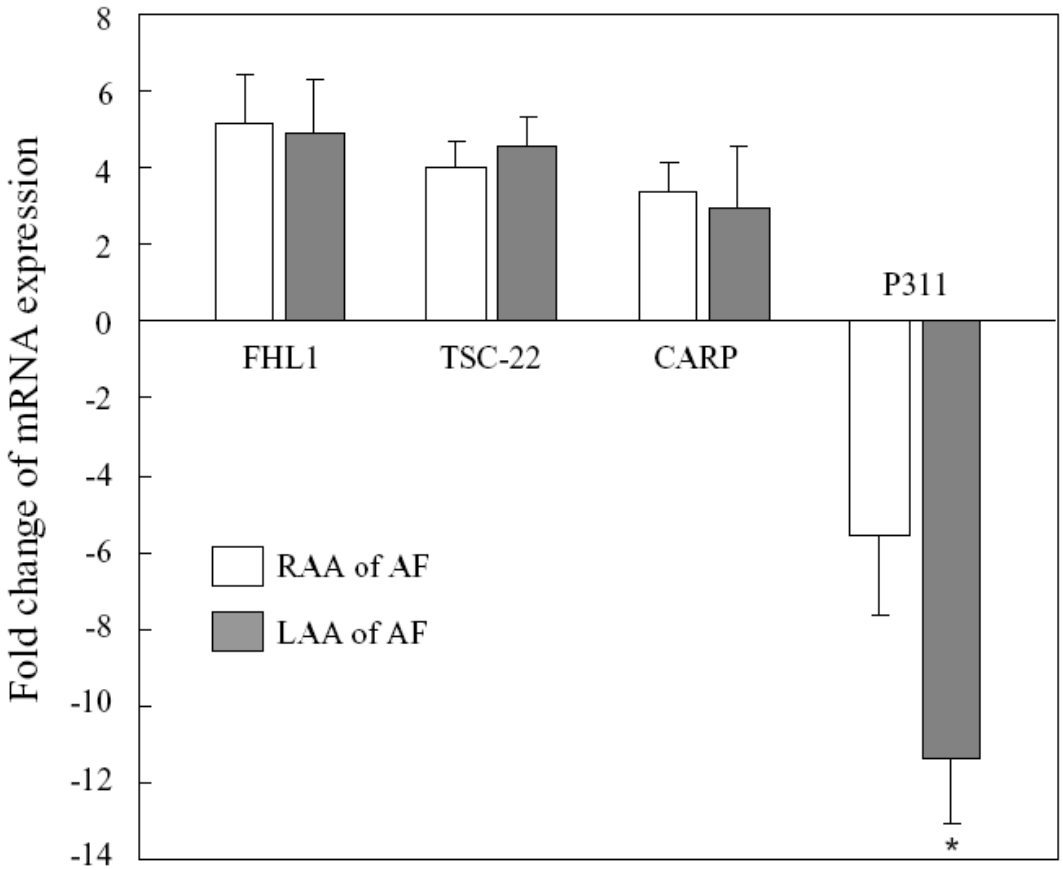

902

903

904

905

906

907

908

909

910

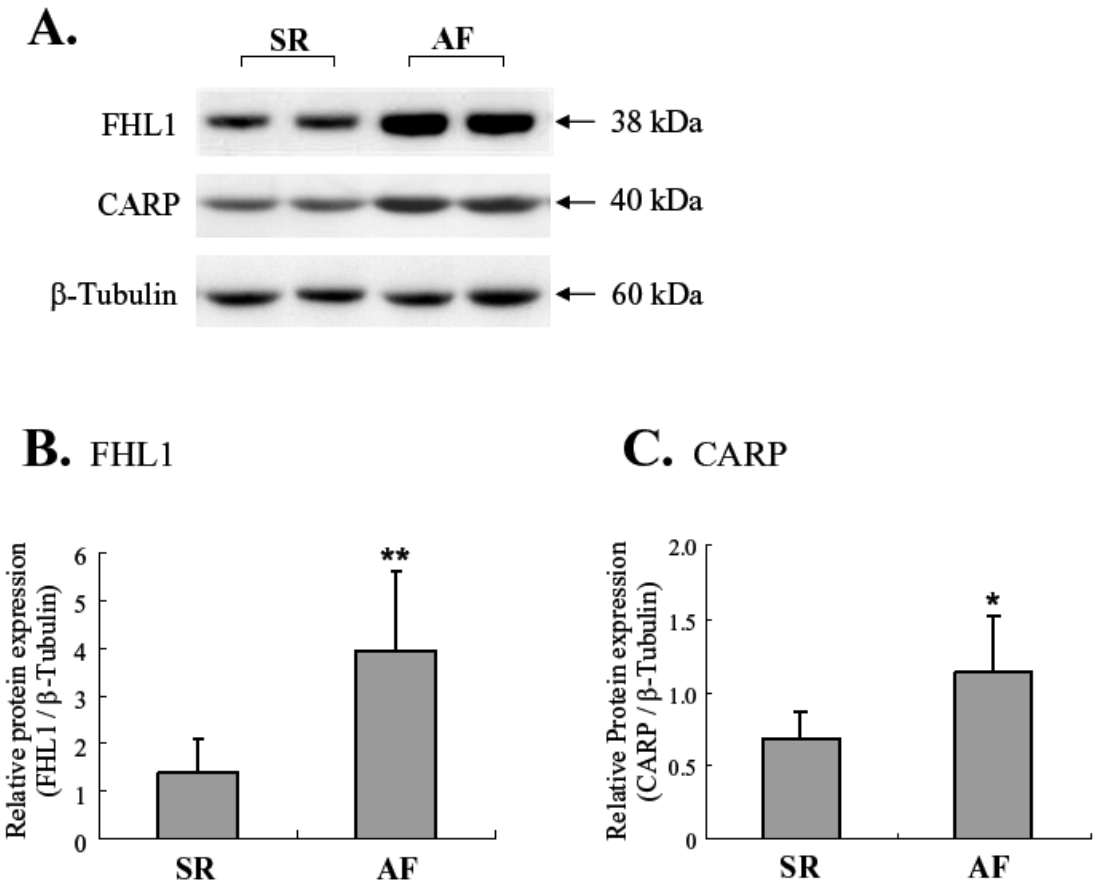

911

912

913

914

915

916

917

918

919

920

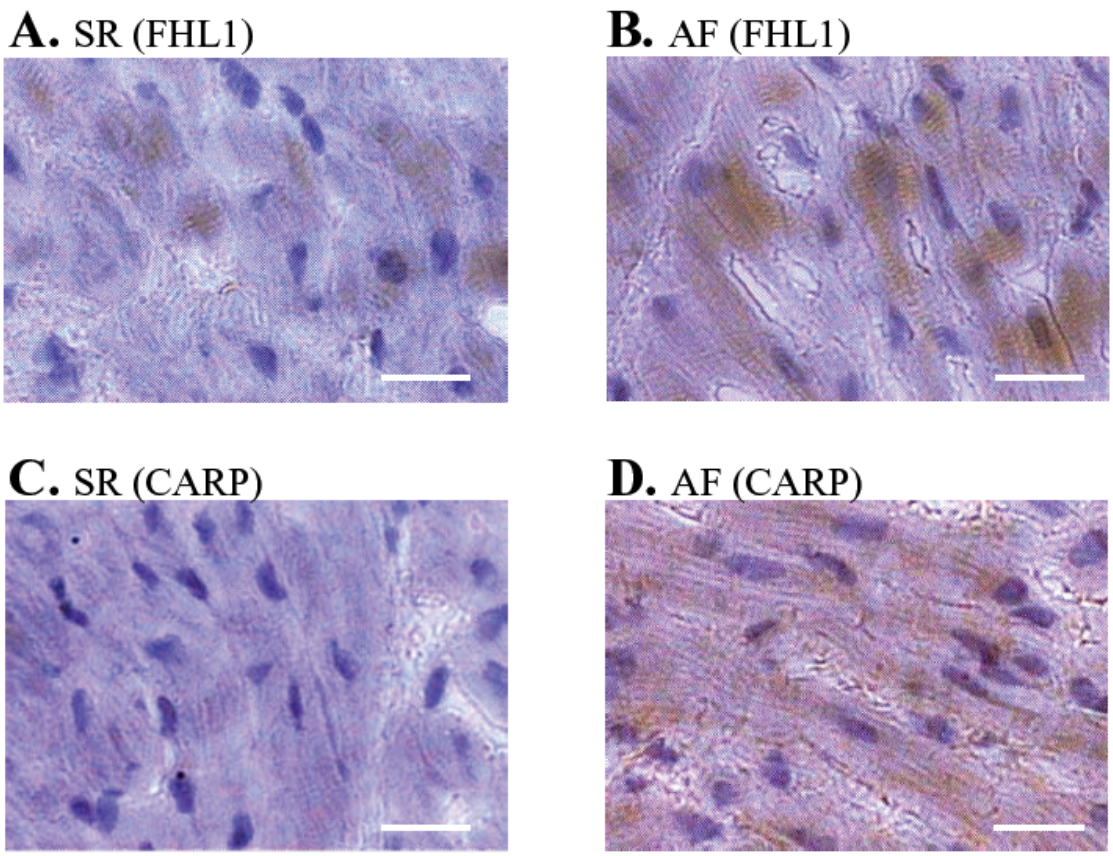

921

922

923

924

925

926

927

928

929

930

931

A. SR

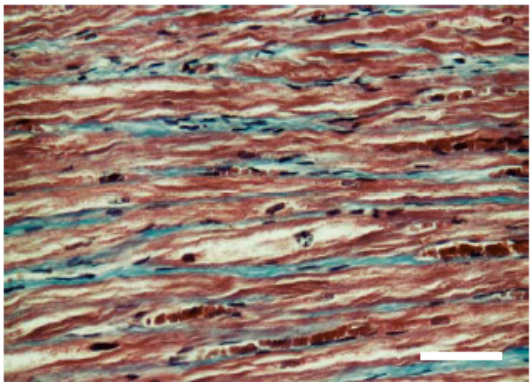

B. AF

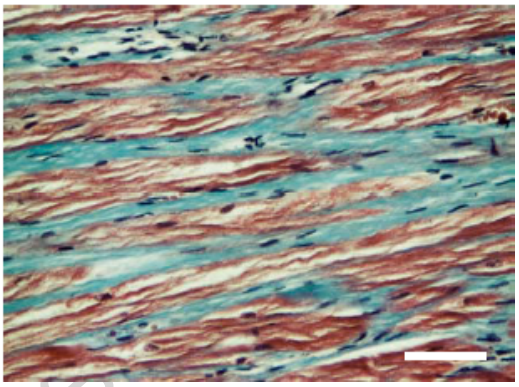

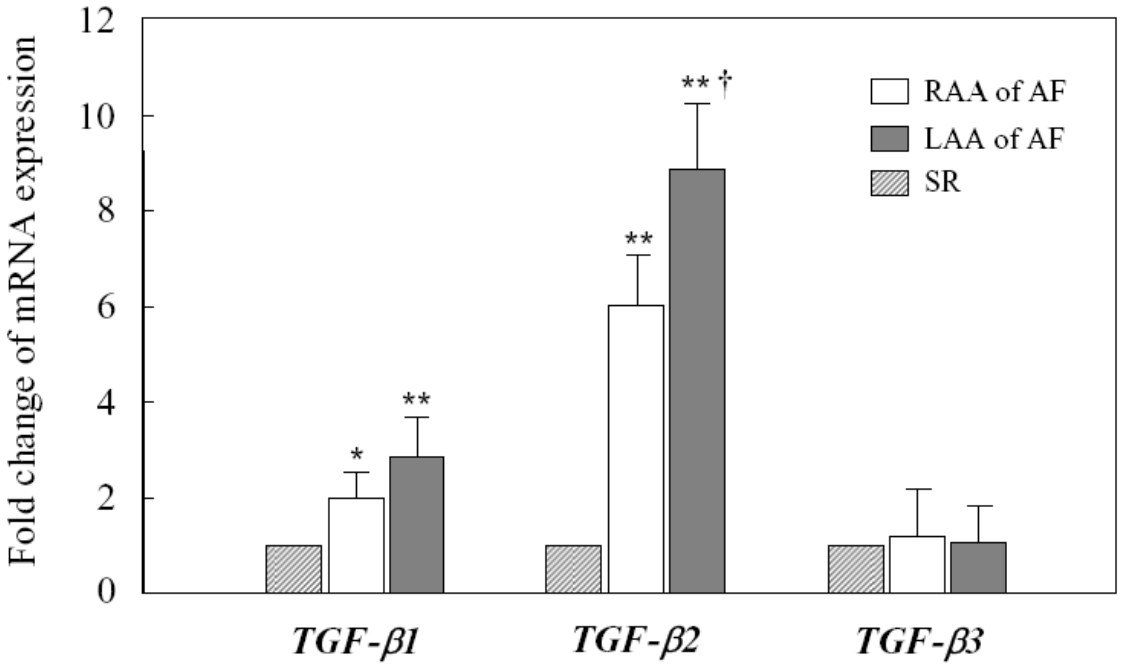

947

948

949

950

951

952

953

954

955

956

957

958

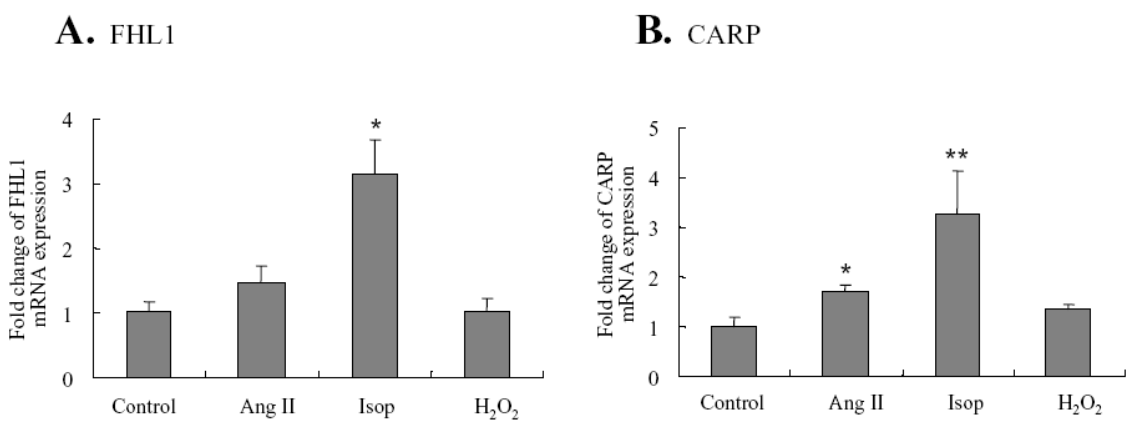

959

960

961

962

963

964

965

966